

Modification of PET Polymer Foil by Na⁺ Implantation

M. TUREK^{a,*}, A. DROŹDZIEL^a, K. PYSZNIAK^a, R. LUCHOWSKI^a,
W. GRUDZIŃSKI^a AND A. KLIMEK-TUREK^b

^aInstitute of Physics, Maria Curie Skłodowska University in Lublin,
Pl. M. Curie-Skłodowskiej 1, 20-031 Lublin, Poland

^bDepartment of Physical Chemistry, Medical University of Lublin, W. Chodźki 4A, 20-093 Lublin, Poland

Very thin (3 μm) polyethylene terephthalate (PET) foils were irradiated with 150 keV Na⁺ ions with the fluences in the range from 1×10^{14} cm⁻² up to 1×10^{16} cm⁻². Modification of chemical structure of the implanted polymer was studied with the Fourier transform infrared and Raman spectroscopies. Destruction of numerous chemical bonds as well as formation of carbon clusters made of *sp*² hybridised C atoms and conducting cluster networks were demonstrated. The increasing presence of chain structures in the graphite-like carbonised layer is pointed out as the *G* band shift and decrease of *D* band could be seen as irradiation fluence rises. The large increase of the modified sample absorbance with the implantation fluence in the UV-VIS region was observed. The decrease of optical band-gap energy from 3.95 eV for the pristine sample down to 0.7 eV for the most heavily treated sample was estimated using the Tauc plot. Reduction of bulk resistivity by more than 8 orders of magnitude is shown in the case of the sample implanted with the fluence 1×10^{16} cm⁻². The sheet resistivity of the sample was also reduced by 5 orders of magnitude. The effect was observed on both sides of the sample, probably as the result of chemical transformations due to local increase of the polymer foil temperature. The moderate increase (15–200%) of the dielectric constant is observed in the frequency range up to 1 MHz and the change rises with the implantation fluence.

DOI: [10.12693/APhysPolA.136.278](https://doi.org/10.12693/APhysPolA.136.278)

PACS/topics: 78.40.Me, 78.30.Jw, 61.82.Pv

1. Introduction

The ion implantation, technique used mainly in microelectronics, has been also applied as a powerful and versatile tool for the surface modification of polymers [1]. These synthetic materials attract attention of scientists and engineers due to their numerous properties including low cost, low density, durability, plasticity etc. [2]. There are, however, some severe limitations of polymer application related to their wear and chemical resistance as well as unpredictable electrical properties [3] and very high electrical resistance restricting their application in electronics. Ion implantation was suggested as a way to change electrical properties of insulating polymers, and even to turn them into semiconductors [4, 5]. Ion implantation is also a very effective tool for improvement of surface properties such as hardness, wear resistance, and wettability [6–8]. It should also be mentioned that ion implantation is one of the ways to make polymer useful for biomedical applications [9, 10]. Indeed, there are other successful techniques allowing efficient modification of polymers, such as electron beam and gamma ray irradiations [11–13].

The modification of physical and chemical surface properties of polymers by implantation is a result of a multitude of processes induced by impinging energetic particles including bond breaking, cross-linking, polymer chain scissions, massive degassing

and carbonisation [4, 14]. Projectiles lose their energy in the host due to nuclear and electronic stopping mechanism. The first process involves energy and momentum transfer in elastic collisions, while the second one results in electron excitation and ionization. The electronic stopping dominates for higher ion energy whereas nuclear stopping plays more important role for lower energies, depending on the projectile/target mass ratio. It is commonly assumed that chain scissioning acts are assigned to the elastic collisions characteristic for nuclear stopping while the electronic energy loss leads to formation of free radicals and the cross-linking in the polymer. The total effect of ion irradiation leading to chain breaking, electron excitation, free radical and dangling bond formation, degassing etc. could be very sensitive to the ratio of nuclear and electronic stopping power [15]. There are numerous reports showing different roles played by both electronic and nuclear stopping in ion implantation modification of polymers. In Ref. [4] it is shown that prevailing electronic stopping leads to intensive dehydrogenation, as well as emission of CO and CO₂ in oxygen containing polymers [1, 16] and carbonisation of the upper layer of the sample. On the other hand, when elastic collisions are of the major importance, one can see that polymer degradation results e.g. in increasing hardness [17]. The chemical reactions occurring in the polymer during the ion implantation are often referred to as an unified process of polymer radiothermolysis [1, 15].

Modification of chemical, physical, tribological, and other properties of a wide variety of polymers by ion implantation has been intensively investigated over many years. These include e.g. polyethylene (PE) [17–20],

*corresponding author; e-mail: mturek@kft.umcs.lublin.pl

polyaryletheretherketone (PEEK) [21, 22], polycarbonate (PC) [23, 24], poly(allyl diglycol carbonate) (CR-39) [25], and polymethylmethacrylate (PMMA) [26, 27]. A lot of effort was also put in studying modification of irradiated elastomers [28–31] and copolymers [32, 33], as well as polyethylene terephthalate (PET).

The latter polymer, polyethylene terephthalate (C₁₀H₈O₄)_n, referred also to by its brand names (Dacron, Laysan, Terylene) is a highly transparent ($\approx 90\%$ in the visible region) strong thermoplastic polymer resin. It is one of the most popular plastics used widely for food and drink packaging purposes as well as for fiber production [34, 35], as magnetic tape carrier and photovoltaic device base [36], for light fibre photographic filters and lens production etc. [37], or concrete reinforcement [38].

The studies of PET sample modifications by ion implantations by noble gases [39–43], metals [44–49], and non-metals [3, 50, 51] have been reported over years. One of the most important changes is a drastic (over many orders of magnitude) decrease of PET resistivity with the implantation fluence. This effect, usually saturating for fluences of the order 10^{16} – 10^{17} cm⁻², is mostly due to massive degassing and carbonisation of the polymer surface layer as well as creation of carbon clusters forming, for higher fluences, a kind of conducting network or percolation cluster [43]. Another commonly observed modification is an increase of absorption in the UV-VIS range and reduction of the optical bandgap energy due to the presence of graphite-like structures. As in the case of other polymers, changes of the surface topography and wettability were also under investigation [52, 53].

The above mentioned changes were also observed in our previous paper describing modification of thin PET foil samples by He, Ne, and Ar irradiation [54]. In this paper the investigations of polymer modification induced by irradiation with light metallic projectiles, namely sodium ions are considered. It was shown [55] using the time of flight secondary ion mass spectroscopy (TOF-SIMS) that experimental Na distribution depth profiles are much wider (by a factor of ≈ 3) than those predicted by the SRIM calculations. That makes an assumption that some bulk effects of the polymer properties modification could be measured in the case of thin foils in even more justified way than previously. The fact that real implantation ranges are comparable to the sample thickness could be especially important in the case of relative dielectric constant measurement using capacitors filled with modified and pristine foils. Changes in the chemical structure of the polymer are studied using the Fourier transform infrared (FTIR) and Raman spectroscopies. Decrease of the irradiated polymer transparency is tested using the UV-VIS spectroscopy that allows to determine changes of the optical bandgap related to the structural modifications of the polymer. The results of measurement of bulk and surface resistivity are also presented in the paper. The above mentioned changes of dielectric constant due to ion implantation are also considered.

2. Experimental

Very thin (3 μm) transparent PET foils (bi-axially oriented, density of ≈ 1.4 g/cm³ supplied by Goodfellow) were implanted with 150 keV beam of Na⁺ ions employing the UNIMAS implanter equipped with an arc discharge ion source with evaporator [56–58], using NaCl as a working substance. Implantations were performed at room temperature with the fluences of 1×10^{14} cm⁻³, 1×10^{15} cm⁻³, and 1×10^{16} cm⁻³. The Na⁺ ion current density of order $1 \mu\text{A}/\text{cm}^2$ was used during the processing. In order to prevent foil from folding and to make all manipulations much easier the foil was placed inside the holder consisting of two cylindrical co-axial teflon rings with internal diameter ≈ 30 mm.

The implanted dopant depth profiles and distributions of vacancies were determined using the SRIM package [59]. The results are shown in Fig. 1. The average projected range was ≈ 400 nm with ≈ 90 nm straggling. The predicted vacancy concentration profile has the maximum at $\approx 80\%$ of that of the dopant. One should, however, bear in mind that the recent TOF-SIMS measurements show that the SRIM predictions should be taken *cum grano salis* as they underestimate the implantation range in polymers [55].

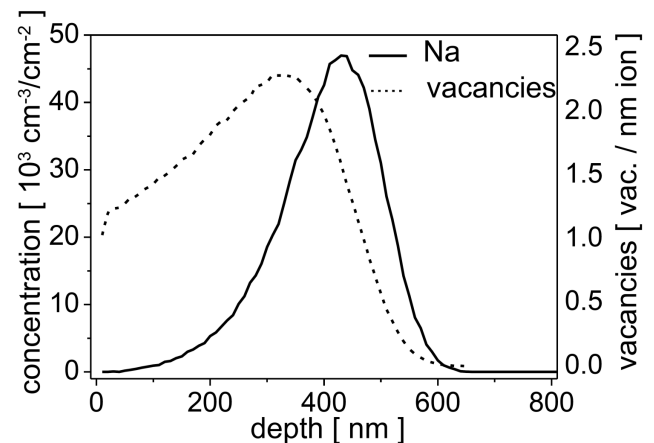


Fig. 1. Sodium atoms and vacancy and depth profiles for 150 keV Na⁺ implantation calculated using SRIM code.

The FTIR spectra of polymer foil samples were measured employing the Nicolet iS50R spectrometer (ThermoScientific, USA). The absorbance spectra in the UV-VIS-NIR range (200–1000 nm) were measured using the Cary 50 (Agilent) spectrophotometer. The Raman spectra (excited by 514 nm line) were collected by the inVia system (Renishaw, UK). Sheet and bulk resistivities of the samples were investigated using the set of coaxial electrodes and the Agilent B2911A precision source/measure unit. The impedance spectroscopy measurements were performed making use of the Hioki IM3570 impedance analyser and the same set of circular electrodes.

3. Results

It is found (e.g. using SRIM package) that the ratio of electronic and nuclear stopping in the case of Na^+ ion implantation into PET is $S_e/S_n = 1.91$. Stopping powers are equal for ion energy ≈ 75 keV. Hence, one may expect that characteristics of effects for both stopping mechanisms may be observed. However, more detailed SRIM calculations (like in [40]) taking into account full cascade collisions using 5000 of incoming primary particles shows that more than 76% of the energy loss is due to the electronic stopping, which was also reported as the dominant stopping mechanism in the case of B^+ implantation into PET [60]. Thus, one may suppose that typical effects for electronic stopping mechanism like degassing and polymer cross-linking are of major importance at least in the topmost modified layer. This is partially confirmed by the fact that intensive gas emission in the target chamber was noticed during the irradiation and polymer darkening visible to the naked eye. Any signs of cracking were detected using either optical or electron microscopy. However, the irradiated foil was very susceptible to wrapping that may suggest shrinking of the top layer.

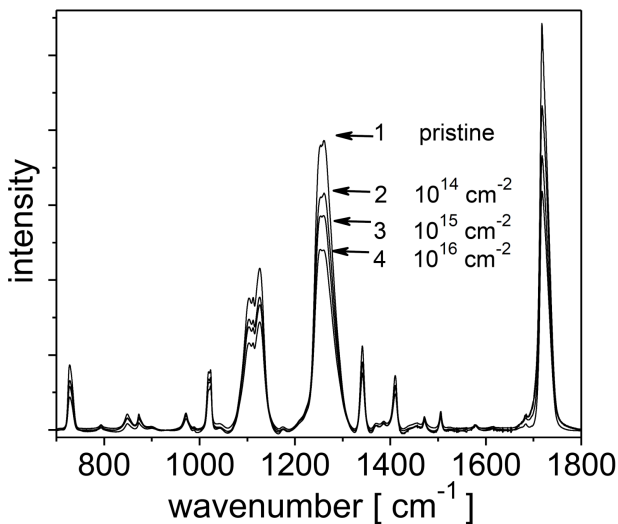


Fig. 2. FTIR spectra of PET samples implanted (Na^+ , 150 keV) with different fluences.

Ion beam irradiation induces severe changes in the chemical structure of the PET foil, as can be seen in the FTIR absorbance spectra shown in Fig. 2. The most prominent signal (and its change) comes from C=O bond stretching (at the carbonyl group) line at ≈ 1117 cm^{-1} . Another example of bond breaking concerns the complex ring (C=C) and O-C stretching peak near 1250 cm^{-1} and also near 1103 cm^{-1} . The intensity of these peaks in the case of the sample irradiated with the highest fluence decreases by $\approx 30\%$ which means that most of these bonds in the subsurface layer is destroyed. Also the peaks at 727 cm^{-1} , 1018 cm^{-1} , corresponding

to different vibration modes of C-H bond, and 1340 cm^{-1} ($-\text{CH}_2$ wagging) decrease with the fluence which confirms the intense dehydrogenation of the irradiated layer.

The Raman spectroscopy also confirms the changes in chemical structure of implanted polymer (see Fig. 3). The main peaks of the spectrum obtained for the pristine sample in the 600 – 1800 cm^{-1} include 632 cm^{-1} C-C-C in-plane ring bending, 857 cm^{-1} C-C breathing, 1097 cm^{-1} and 1118 cm^{-1} C-O stretching plus $-\text{CH}$ in-plane bending, 1286 cm^{-1} ring plus O-C stretching, 1613 cm^{-1} C=C ring stretching and 1727 cm^{-1} C=O stretching [61]. Even for the smallest fluence the destruction of chemical bonds in the subsurface layer of the polymer is visible, the peaks corresponding to C=C ring and 1727 cm^{-1} C=O stretching, are the only distinct ones. The peak height reduction is much stronger than that observed for PET implanted with noble gases [54]. As the fluence increases to 10^{15} cm^{-2} the polymer characteristic peaks disappear, whilst wide bands near 1600 cm^{-1} and a smaller one at ≈ 1350 cm^{-1} appear. These are *G* and *D* bands being the fingerprints of graphite-like structures built of sp^2 hybridised carbon atoms. The sp^2 hybridised C atoms are known to form clusters/island in the sp^3 matrix [43]. The sp^2 clusters are made of chains and ring structures interconnected and linked to each other. The above mentioned *D* and *G* bands induced by ion beam processing are the signs of breathing vibrations of sp^2 carbon atoms rings (*D*) and stretching vibration modes of both rings and carbon chains (*G*). It should be kept in mind that the closest is the *G* band maximum to its pure graphite position (1582 cm^{-1}), the higher is the content of aromatic rings in the cluster structure. Hence, as the *G* band position shifts to ≈ 1540 cm^{-1} (for $\Phi = 10^{16}$ cm^{-2}) and the *D* band is barely visible, one may conclude that the content of chain-like structures in irradiated polymer increases with implantation dose. It should be pointed out that the Raman spectra were collected from the topmost layer of the polymer which became degassed and carbonized mostly due to the electronic stopping energy transfer.

On the other hand, polymers with substituents heavier than H have larger tendency to scission and bond breaking, and such behaviour in deeper lying layers, where projectiles have lower energy and nuclear stopping prevails, is visible as the lowering peaks in the FTIR spectra. On the other hand, the decrease of C=O peaks which may be assigned both to the degassing and chain scission, and the decrease of benzene ring modes may suggest transformation of these structures, e.g. in the graphite-like clusters. However, the fact that any signs of embrittlements, cracks, or powderisation of the polymer were observed using optical and scanning electron microscopies (OM, SEM) may lead to the conclusion that the polymer degradation due to chain scission is not the most important mechanism of structural modification in the considered case. To summarise things up — the presence of the signatures of carbon structures (*D* and *G* bands)

in the Raman spectra that were collected from the top layer of the foil suggest the strong presence of electronic stopping leading to intensive degassing and formation of C clusters/networks due to cross-linking. It should be mentioned that the lack of *D* and *G* bands in the spectra obtained for 50 keV B⁺ irradiated PET samples [60] was explained by the fact that low energy projectile was not able to destroy the ring structure. In the currently considered case electronic stopping initially prevails and leads to degassing and formation of carbon structures in the upper layer of the foil. Although, the importance of nuclear stopping increases as projectiles slow down in deeper layers, which leads to bond breaking visible in the FTIR spectra that was collected from the whole cross-section of the modified foil.

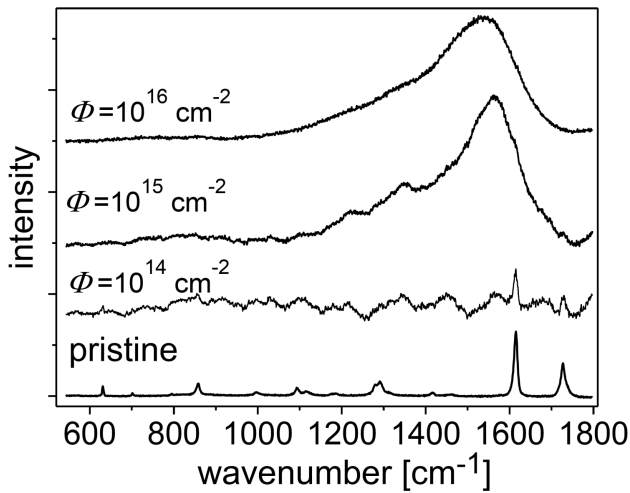


Fig. 3. Raman spectra for the samples implanted with different fluences of Na ions.

The unimplanted PET foil is almost transparent in the visible region which is confirmed by the UV-VIS spectra in the range 300–800 nm which can be seen in Fig. 4. The carbonisation of the sample due to ion implantation can be seen even with the naked eye as its darkening. More details about the relations between the sample colour and its band structure could be found in [43]. For the implantation fluences larger than 10^{15} cm^{-2} a large increase of the absorbance could be seen as well as the shift of the absorption edge towards larger wavelengths as in the case of noble gas implantation [54]. Both these effects are due to the formation of conduction carbon cluster structures related to the decrease of the optical bandgap of the modified sample which was also seen in Ref. [27, 40–42]. Assuming that one deals with indirect allowed transition in the case of PET, the optical bandgap E_o can be deduced using the Tauc approach

$$\alpha h\nu \sim (h\nu - E_o)^2, \quad (1)$$

where α is the absorption coefficient. The optical bandgap can be estimated by plotting $(\alpha h\nu)^{1/2}$ vs. $h\nu$ and taking the interception of the linear part of the plot

and the $h\nu$ axis (see Fig. 4a) The estimated values of the bandgap energy for the samples are presented in Table I. As one may expect, due to the changes of polymer chain structure, formation of carbonaceous clusters and cluster network, and appearance of lower-energy lying states due to the ion implantation [27, 62], the bandgap energy decreases with the implantation fluence. The bandgap energy in the case of $\Phi = 10^{16} \text{ cm}^{-2}$ is reduced to 0.7 eV only, compared to $\approx 3.95 \text{ eV}$ in the case of the pristine sample.

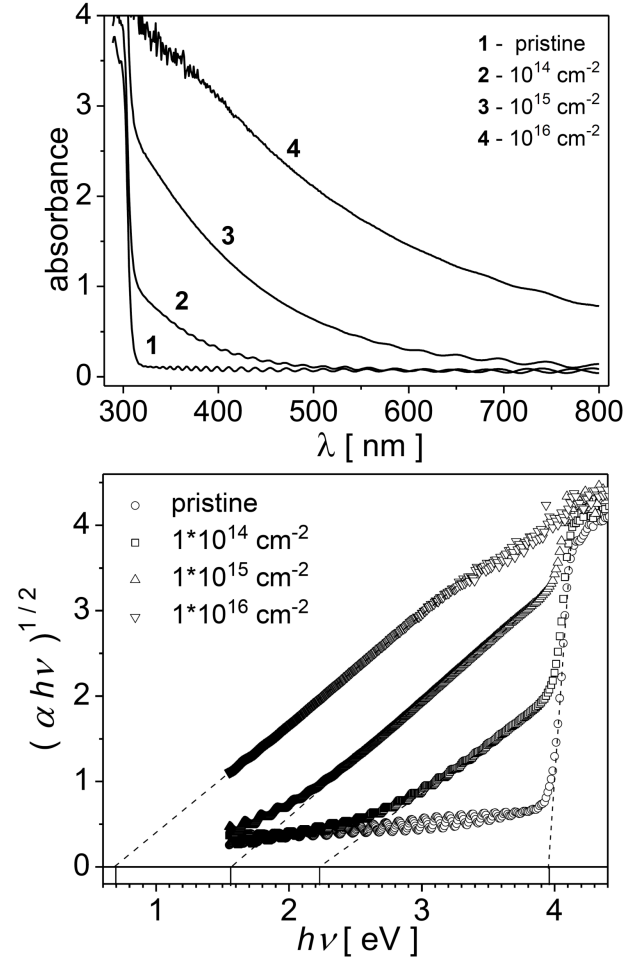


Fig. 4. UV-vis absorbance spectra (a) and Tauc plots (b) for the samples implanted with different fluences.

TABLE I

Optical bandgap energies estimated using the Tauc approach and the average carbon cluster sizes for different Na⁺ irradiation fluences

$\Phi [\text{cm}^{-2}]$	$E_o [\text{eV}]$	N
pristine	3.96	–
1×10^{14}	2.22	240
1×10^{15}	1.55	490
1×10^{16}	0.7	2400

The shape of the absorption spectrum in the case of heavily modified samples is determined mostly due to the absorption by the π -bonded C clusters and the shift of the absorption edge comes from the clusters increase. There are several approaches that allow estimation of the size of the carbon clusters from the optical absorption data [63–65]. Using that presented in [65] one can estimate the mean number of C atoms in a cluster (N) by the following equation:

$$N = \left(\frac{34.3}{E_o [\text{eV}]} \right)^2. \quad (2)$$

Looking at the data in Table I it can be easily seen that the number of C atoms in the cluster rises with the implantation fluence. For low dose implantation conducting carbon clusters could be regarded as isolated. As the fluence increases the size of clusters increases, reaching more than 1000 atoms, and the clusters start to aggregate forming a vast conducting network in a subsurface layer that changes electrical properties of the sample [40, 41, 62].

This is also observed in the presented case of Na implanted PET foils. It should be kept in mind that considering the bulk resistivity modification is justified in the case of a very thin foil implanted using light projectiles as the projected range and the depth of the modified layer should be comparable to the sample thickness. Figure 5 shows the bulk conductivity of PET foils as a function of implantation fluence. One can see that the resistance of the sample falls dramatically with the irradiation fluence, by \approx more than 8 orders of magnitude in the considered fluence range. It should be mentioned that a similar effect was observed for the samples irradiated with different projectiles, including noble gases [40–43], metals [44–49], and non-metals [3, 50, 51]. The bulk resistivity reduction due to Na implantation is stronger than that reported for the PET samples irradiated with light noble gases [54]. This may be due to the fact that metallic precipitates are known to be formed in the implanted polymers and such “conducting islands” also contribute to the change of sample resistivity [2, 4, 5].

The sheet resistivity of the samples was also measured and the results are shown in Fig. 6. One can see that the sheet resistivity is reduced by almost 5 orders of magnitude in the case of the most modified sample. It should be noted that saturation is observed for $\Phi \approx 10^{16} \text{ cm}^{-2}$. Such fluences and further modifications concern mostly the deeper layers of the foil because the surface of the polymer is totally modified. The resistivity of the reverse side of the foil is also dramatically reduced. The probable explanation is that the very thin polymer foil has much lower thermal stability than the bulk material. A role may be also played by dopant diffusion which can influence the dopant depth profile in polymers [4, 5], especially in the case of light projectiles. To a certain degree it could explain the discrepancies of experimental Na^+ distributions

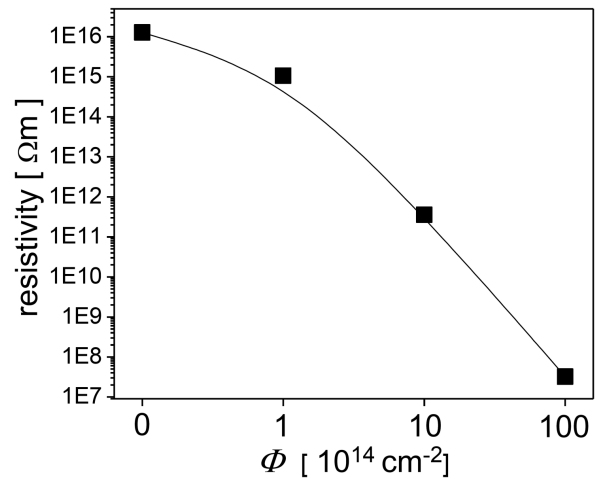


Fig. 5. Changes of PET foil bulk resistance with the Na^+ implantation fluence.

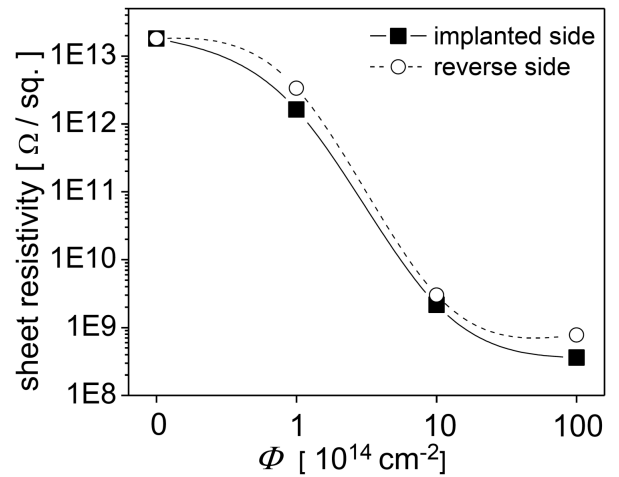


Fig. 6. Sheet resistivity for the samples implanted with different Na^+ fluences measured on both sides of foils.

from that predicted using SRIM [59]. The sheet resistivity on the reverse side is only ≈ 2 times higher than that of the implanted side. In the case of noble gas implantations [54] the sheet resistivity on the reverse side was more than 2 orders of magnitude higher than that on the implanted one, still noticeably lower than the pristine sample resistivity.

Changes of the real part of electric constant due to ion implantation were determined by comparing the capacities of the condenser filled with the implanted and pristine samples: ε and ε_p , respectively. The results for the frequencies up to 1 MHz are presented in Fig. 7. One can see that moderate dose implantations change the dielectric constant by 30% ($\Phi = 10^{15} \text{ cm}^{-2}$). No frequency dispersion is observed in these cases. Some frequency dispersion can be seen for the sample implanted with the highest dose. For $\Phi = 10^{16} \text{ cm}^{-2}$ the relative dielectric constant increases twice (compared to the unmodified sample) in the low frequency region and drops to 1.35 for f larger than 100 kHz. These results are

comparable to the changes induced by He ions implantations, and much smaller than the impact of heavier noble gas ion irradiation on the dielectric constant (even factor of 12 in the case of Ar⁺ bombardment).

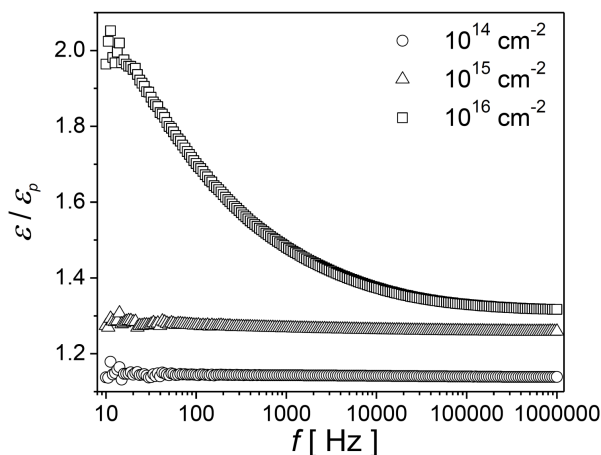


Fig. 7. Changes of the relative dielectric constant of the PET samples implanted with different fluences of Na.

4. Conclusions

The paper presents the investigations of modification of structural, optical, and electrical properties of PET foils caused by Na⁺ implantation with the energy 150 keV and the fluences from 10¹⁴ cm⁻² up to 10¹⁶ cm⁻². The destruction of different bonds in the polymer chains was demonstrated using the Raman and FTIR spectroscopies as well as the fact that the degree of destruction increases with the irradiation fluence. The analysis of the Raman spectra indicates formation of carbon clusters composed of sp² hybridised atoms as strong wide D and G bands characteristic of the amorphous carbon structures are present. Changes of the absorbance in the UV-VIS range are due to the increasing carbon cluster size and formation of vast conducting network with the implantation fluence. This results in decrease of the optical bandgap down to 0.7 eV ($\Phi = 10^{16}$ cm⁻²) and also leads to the dramatical reduction of electrical resistivity of the modified samples — even by more than 8 orders of magnitude for most of modified samples. The average sizes of C clusters were also estimated from the bandgap energy shift — the number of C atoms in a cluster is found to rise with Φ reaching more than 2000 for the maximum fluence. It was also demonstrated that the sheet resistivity of the implanted foils is reduced up to 5 orders of magnitude. The reduction of sheet resistivity was also observed on the reverse (unimplanted) side of the thin foil, albeit not as strong as on the implanted one (factor of 2). This effect is most probably due to the intensive heating of the thin foil during irradiation leading to chemical modification of the deeper layers. The relative dielectric constant of the implanted foils was measured

in the range up to 1 MHz. The constant becomes larger with the implantation fluence in the considered f range by 15–30% in the case of moderate fluence implantations, and by 200% in the case of $\Phi = 10^{16}$ cm⁻² in the low f range. These changes are comparable to those obtained using light noble gas ion irradiations.

References

- [1] D.V. Sviridov, in: *Chemical Problems of the Development of New Materials and Technologies*, Ed. O.A. Ivashkevich, Belarusian State University, Minsk 2003, p. 88.
- [2] Y. Wu, T. Zhang, H. Zhang, X. Zhang, Z. Deng, G. Zhou, *Nucl. Instrum. Methods Phys. Res. B* **169**, 89 (2000).
- [3] Y. Wu, T. Zhang, A. Liu, X. Zhang, G. Zhou *Sci. China E* **46**, 125 (2003).
- [4] V. Popok, *Rev. Adv. Mater. Sci.* **30**, 1 (2012).
- [5] T. Venkatesan, L. Calcagno, B.S. Elman, G. Foti, in: *Ion Beam Modification of Insulators*, Ed. P. Mazzoldi, G.W. Arnold, Elsevier, Amsterdam 1987, p. 301.
- [6] E.H. Lee, *Nucl. Instrum. Methods Phys. Res. B* **151**, 29 (1999).
- [7] N. Shekhawat, S. Aggarwal, A. Sharma, K.G.M. Nair, *J. Macromol. Sci. B* **55**, 652 (2016).
- [8] Y. Kim, Y. Lee, S. Han, K.J. Kim, *Surf. Coat. Technol.* **200**, 4763 (2006).
- [9] O. Nedela, P. Slepicka, V. Svorcik, *Materials* **10**, 1115 (2017).
- [10] A. Kondyurin, M. Bilek, *Ion Beam Treatment of Polymers, Applications Aspects from Medicine to Space*, Elsevier, Amsterdam 2008.
- [11] Z. Zimek, G. Przybytniak, A. Nowicki, *Radiat. Phys. Chem.* **81**, 1398 (2012).
- [12] B. Nayak, S. Acharya, D. Bhattacharjee, R.I. Bakhtsingh, R. Rajan, D.K. Sharma, S. Dewangan, V. Sharma, R. Patel, R. Tiwari, S. Benarjee, S.K. Srivastava, *J. Instrumentat.* **11**, P03006 (2016).
- [13] G. Przybytniak, E.M. Kornacka, K. Mirkowski, M. Walo, Z. Zimek, *Nukleonika* **53**, 89 (2008).
- [14] M. Guenther, G. Gerlach, G. Suchanek, K. Sahre, K.J. Eichhorn, B. Wolf, A. Deineka, L. Jastrabik, *Surf. Coat. Technol.* **158**, 108 (2002).
- [15] R. Mikšová, A. Macková, H. Pupikova, P. Malinský, P. Slepicka, V. Švorčík, *Nucl. Instrum. Methods Phys. Res. B* **406**, 199 (2017).
- [16] D.V. Sviridov, *Russ. Chem. Rev.* **74**, 315 (2002).
- [17] A. Tuross, J. Jagielski, A. Piątkowska, D. Bieliński, L. Ślusarski, N.K. Madi, *Vacuum* **70**, 201 (2003).
- [18] A. Valenza, A.M. Visco, L. Torrisi, N. Campo, *Polymer* **45**, 1707 (2004).
- [19] M. Nenadović, J. Potocnik, M. Ristić, S. Strbac, Z. Rakocević, *Surf. Coat. Technol.* **206**, 4242 (2012).
- [20] D.M. Bieliński, C. Ślusarczyk, J. Jagielski, P. Lipiński, *Polimery* **52**, 329 (2007).
- [21] E.A. Wakelin, A. Fathi, M. Kracica, G.C. Yeo, S.G. Wise, A.S. Weiss, D.G. McCulloch, F. Dehghani, D.R. McKenzie, M.M. Bilek, *ACS Appl. Mater. Interfaces* **7**, 23029 (2015).

- [22] F. Awaja, D.V. Bax, S. Zhang, N. James, D.R. McKenzie, *Plasma Process. Polym.* **9**, 355 (2012).
- [23] P.K. Goyal, V. Kumar, R. Gupta, S. Kumar, P. Kumar, D. Kanjilal, *AIP Conf. Proc.* **1349**, 543 (2011).
- [24] V. Resta, L. Calcagnile, G. Quarta, L. Maruccio, A. Cola, I. Farella, G. Giancane, L. Valli, *Nucl. Instrum. Meth. Phys. Res. B* **312**, 42 (2013).
- [25] N. Shekhawat, *Adv. Mater. Res.* **665**, 214 (2013).
- [26] M.C. Salvadori, M. Cattani, F.S. Teixeira, I.G. Brown, *Appl. Phys. Lett.* **93**, 073102 (2008).
- [27] S. Arif, M.S. Rafique, F. Saleemi, R. Sagheer, F. Naab, O. Toader, A. Mahmood, R. Rashid, M. Mahmood, *Nucl. Instrum. Methods Phys. Res. B* **358**, 236 (2015).
- [28] S. Rosset, M. Niklaus, P. Dubois, H.R. Shea, *Adv. Funct. Mater.* **19**, 470 (2009).
- [29] J. Jagielski, D. Grambole, I. Jozwik, D.M. Bielinski, U. Ostaszewska, D. Pieczynska, *Mater. Chem. Phys.* **127**, 342 (2011).
- [30] J. Jagielski, U. Ostaszewska, D. Bielinski, A. Piatkowska, M. Romaniec, *Acta Phys. Pol. A* **123**, 888 (2013).
- [31] X. Zhou, X. Chen, T.C. Mao, X. Li, X.H. Shi, D.L. Fan, Y.M. Zhang, *Plast. Reconstr. Surg.* **137**, 690e (2016).
- [32] A. Kondyurin, M. Bilek, A. Janke, M. Stamm, V. Luchnikov, *Plasma Process. Polym.* **5**, 155 (2008).
- [33] K. Kim, W. Sung, H.J. Park, Y. Lee, S. Han, W. Kim, *J. Appl. Polym. Sci.* **92**, 2069 (2004).
- [34] C. Alvarez, I. Sics, A. Nogales, Z. Dencheva, S.S. Funari, T.A. Ezquerro, *Polymer* **45**, 3953 (2004).
- [35] *Handbook of Fiber Science and Technology Vol. 2: Chemical Processing of Fibers and Fabrics*, Ed. M. Lewin, Routledge 2018.
- [36] C.S. Goh, S.C. Tan, S.L. Ngoh, J. Wei, *Energy Proced.* **15**, 428 (2012).
- [37] M. Mallick, T. Patel, R.C. Behera, S.N. Sarangi, S.N. Sahu, R.K. Choudhry, *Nucl. Instrum. Methods Phys. Res. B* **248**, 305 (2006).
- [38] J.M. Irwan, S.K. Faisal, N. Othman, I. Mohamad, H. Wan, R.M. Asyraf, M.M.K. Annas, *Adv. Mater. Res.* **795**, 352 (2013).
- [39] M. Djebara, J.P. Stoquert, M. Abdesselam, D. Muller, A.C. Chami, *Nucl. Instrum. Methods Phys. Res. B* **274**, 70 (2012).
- [40] P.K. Goyal, V. Kumar, R. Gupta, S. Mahendia, A.S. Kumar, *Adv. Appl. Sci. Res.* **2**, 77 (2011).
- [41] R. Kumar, M. Goyal, A. Sharma, S. Aggarwal, A. Sharma, D. Kanjilal, *AIP Conf. Proc.* **1661**, 110010 (2015).
- [42] M. Chawla, R. Rubi, R. Kumar, A. Sharma, S. Aggarwal, P. Kumar, D. Kanjilal, *Adv. Mater. Res.* **665**, 221 (2013).
- [43] A. Tóth, M. Veres, K. Kereszturi, M. Mohai, I. Bertóti, J. Szépvölgyi, *Appl. Surf. Sci.* **257**, 10815 (2011).
- [44] M.G. Lukashevich, V.N. Popok, V.S. Volobuev, A.A. Melnikov, R.I. Khaibullin, V.V. Bazarov, A. Wieck, V.B. Odzhaev, *Open Appl. Phys. J.* **2**, 1 (2009).
- [45] Z.J. Han, B.K. Tay, *J. Appl. Polym. Sci.* **107**, 3332 (2008).
- [46] Y.A. Bumai, V.S. Volobuev, F. Valeev, N.I. Dolgikh, M.G. Lukashevich, R.I. Khaibullin, V.I. Nuzhdin, V.B. Odzhaev, *J. Appl. Spectrosc.* **79**, 773, (2012).
- [47] Y. Wu, T. Zhang, Y. Zhang, H. Zhang, H. Zhang, G. Zhou, *Sci. China E* **44**, 493 (2001).
- [48] P. Malinsky, A. Mackova, V. Hnatowicz, R.I. Khaibullin, V.F. Valeev, P. Slepicka, V. Svorcik, M. Slouf, V. Perina, *Nucl. Instrum. Methods Phys. Res. B* **272**, 396 (2012).
- [49] Y. Wu, T. Zhang, Z. Yi, X. Zhang, H. Zhang, X. Zhang, C. Zhou, in: *Proc. 6th Int. Conf. on Solid-State and Integrated-Circuit Technol.*, 2001, p. 1464.
- [50] Y.A. Bumai, V.S. Volobuev, F. Valeev, N.I. Dolgikh, M.G. Lukashevich, R.I. Khaibullin, V.I. Nuzhdin, V.B. Odzhaev, *J. Appl. Spectrosc.* **79**, 773 (2012).
- [51] V. Kumar, R.G. Sonkawade, S.K. Chakarvarti, P. Singh, A.S. Dhaliwal, *Radiat. Phys. Chem.* **81**, 65 (2012).
- [52] P.L. Sant'Ana, J.R.R. Bortoleto, N.C. da Cruz, E.C. Rangel, S.F. Durrant, *Rev. Bras. Apl. Vac.* **36**, 68 (2017).
- [53] M. Drabik, K. Dworecki, R. Tańczyk, S. Wąsik, J. Żuk, *Vacuum* **81**, 1348 (2007).
- [54] A. Drożdźiel, M. Turek, K. Pyszniak, S. Prucnal, R. Luchowski, W. Grudziński, A. Klimek-Turek, J. Partyka, *Acta Phys. Pol. A* **132**, 264 (2017).
- [55] Y. Kudriavtsev, A.G. Hernández, R. Asomoza, V.M. Korol, *Surf. Interf. Anal.* **49**, 1049 (2017).
- [56] M. Turek, A. Drożdźiel, K. Pyszniak, S. Prucnal, *Nucl. Instrum. Meth. Phys. Res. B* **269**, 700 (2011).
- [57] M. Turek, A. Drożdźiel, K. Pyszniak, S. Prucnal, J. Żuk, *Przegląd Elektrotechniczny* **86**, 193 (2010).
- [58] M. Turek, A. Drożdźiel, K. Pyszniak, S. Prucnal, D. Mączka, Y. Yushkevich, A. Vaganov, *Instrum. Exp. Techn.* **55**, 469 (2012).
- [59] J.F. Ziegler, M.D. Ziegler, J.P. Biersack, *Nucl. Instrum. Meth. Phys. Res. B* **268**, 1818 (2010).
- [60] A. Sharma, M. Chawla, D. Gupta, R. Kumari, M. Bura, N. Shekhawat, S. Aggarwal, *Vacuum* **159**, 306 (2019).
- [61] T. Lippert, F. Zimmermann, A. Wokaun, *Appl. Spectrosc.* **47**, 1931 (1993).
- [62] V. Kumar, R.G. Sonkawade, S.K. Chakarvarti, P. Singh, A.S. Dhaliwal, *Radiat. Phys. Chem.* **81**, 65 (2012).
- [63] I.P. Kozlov, V.B. Odzhaev, I.A. Karpovich, V.N. Popok, D.V. Sviridov, *J. Appl. Spectrosc.* **65**, 390 (1998).
- [64] S.A. Nouh, M.H. Abdul-Salem, A. Ahmed Morsy, *Radiat. Meas.* **37**, 25 (2003).
- [65] S. Gupta, D. Choudhary, A. Sarma, *J. Polym. Sci. B Polym. Phys.* **38**, 1589 (2000).